

Investigation of a Robust Method for Connecting Dissimilar 3D Finite Element Models

by

David M. Trujillo¹

December 2005

¹ Consultant, TRUCOMP, Fountain Valley, California
trucomp@earthlink.net

Abstract

A robust method for connecting independently meshed three dimensional finite element heat conduction models is investigated numerically. Two three dimensional heat conduction models with dissimilar meshes are investigated. one with a direct coupling connection and the other with a thermal contact resistance.. A Delaunay triangulation method is used to construct a mesh at the interface in order to accurately perform the numerical integration of the contact matrix.

Key Words: finite elements, dissimilar meshes, three dimensional, contact resistance, heat conduction, Delaunay triangles.

1.0 Introduction

A frequent problem in thermal analysis is to connect separately meshed three dimensional finite element heat conduction models of components either directly or with a surface contact resistance. These components may have been previously meshed or constructed by different analysts or they have been meshed differently to reflect their unique characteristics. This paper investigates a method for connecting dissimilar meshes. The method is very robust in that the meshes do not have to line up in any prescribed manner. The computations are outlined and two examples are included to illustrate the effectiveness of the method.

The availability of a general contact resistance element will greatly facilitate the assemblage of finite element models. Each component of a model can be meshed separately without having to design or modify the mesh in order to connect to other components. This is an advantage in that standard components can be meshed once and assembled as required, especially in a design mode where components are being moved relative to each other. This approach offers a much simpler approach than the more difficult problem of meshing the entire model with the imposed constraints that the meshes of separate parts match at the connecting surfaces.

The method investigated here is an extension of the approach taken in Reference [1]. There are many different approaches for connecting dissimilar finite element meshes [2-6] for both linear elasticity and elliptic models. The method in this paper uses only standard finite element methodology and does not use Lagrange multipliers or artificial weighting parameters. The method can be easily incorporated into existing finite element heat conduction programs. Although the method is applicable to transient models this paper investigates only steady state three dimensional heat conduction models. The purpose is to show how complicated meshes can be

accurately joined in a robust and efficient manner.

2.0 The General Method

This method was presented in Reference [1] and is repeated here for the sake of convenience. Consider two surfaces, **A** and **B**, each in a x-y plane(Figure 1). Each of these surfaces can have its own pattern of nodes and elements. These surfaces should be thought of as the contact surfaces between two dissimilar three dimensional models. The problem is to connect these surfaces in the z direction with a contact resistance. The heat transfer between the surfaces does not depend on the dimension z and in practice the surfaces are either touching or the distance between them is very small. In this case, a contact resistance is used to calculate the heat transfer between the surfaces, typical units are Watts/m²/K (BTU/ft²/hr/F). Thermal contact resistance is a physical constant primarily caused by the imperfect contact between two surfaces. It is usually derived empirically and depends on many variables including material types and contact pressure.

This method is based on the idea of constructing a general three dimensional conduction element between the surfaces but with only a thermal conductivity in the z direction. The thermal conductivities in the x and y direction are zero. The formulation will assume that surface **A** is the same or smaller than **B** and is projected directly onto **B** (Figure 1). With these assumptions the three dimensional temperature distribution in this element is assumed to be

$$T(x,y,z) = (1 - z) T_a(x,y) + zT_b(x,y) \quad \text{where } 0 \leq z \leq 1 \quad (1)$$

The two dimensional temperature distributions, $T_a(x,y)$ on surface **A** and $T_b(x,y)$ on surface **B**, are uniquely determined by the elements and nodes on each of the respective contact surfaces of the three dimensional models. The depth of the element in the z direction can be arbitrary set to

1.0. In this manner, the general element represents a continuous temperature between the two surfaces.

The overall goal is to compute a conductance matrix \mathbf{K} representing the heat transfer in the z direction. This conductance matrix will involve nodes on both surfaces and is of the general form.

$$\mathbf{KT} = \mathbf{c} \begin{bmatrix} \mathbf{K}_{11} & \mathbf{K}_{12} \\ \mathbf{K}_{12}^T & \mathbf{K}_{22} \end{bmatrix} \begin{bmatrix} \mathbf{T}_a \\ \mathbf{T}_b \end{bmatrix} \quad (2)$$

\mathbf{T}_a and \mathbf{T}_b are vectors representing the nodes on surface \mathbf{A} and \mathbf{B} , respectively. \mathbf{c} is the thermal contact resistance coefficient. There is no restriction on how many nodes or elements are on each surface. The elements can be of any type and there does not have to be any relationship between the two surfaces.

In calculating a conductance finite element, the temperature distribution in the element is usually expressed in terms of general three dimensional shape functions $N_i(x,y,z)$ and the nodal temperatures T_i for this element.

$$T(x,y,z) = T_1 N_1(x,y,z) + T_2 N_2(x,y,z) + \dots + T_n N_n(x,y,z) \quad (3)$$

where n is the total number of nodes in the interface element. For the case of surface \mathbf{A} projecting onto surface \mathbf{B} , the total number of nodes is equal to the total number on surface \mathbf{A} (m) plus all the nodes on surface \mathbf{B} ($n-m$) influenced by the projection. All nodes connected to any element on \mathbf{B} that are influenced by the projection are included in surface \mathbf{B} .

If the shape functions were known, then the entries \mathbf{k}_{ij} of the conductance matrix would be easily computed, for the case of conductivity only in the z direction, as [7]

$$k_{ij} = c \int_{\text{volume}} \frac{\partial N_i}{\partial z} \frac{\partial N_j}{\partial z} dx dy dz \quad (4)$$

where c is the thermal contact resistance coefficient.

It is also possible to express the temperatures on surface **A** and **B** in terms of their own unique shape functions $S_i(x,y)$ and nodal temperatures. For surface **A**

$$T_a(x,y) = T_1 S_1(x,y) + T_2 S_2(x,y) + \dots + T_m S_m(x,y) \quad (5)$$

where m is the total number of nodes in surface **A**. A similar expression, $T_b(x,y)$, can be written for surface **B**. The two dimensional shape functions $S_i(x,y)$ represent the temperature distribution over a surface with T_i set to unity and all the other nodal temperatures set to zero. With these expressions the conductance matrix entries in Equation (4) can be evaluated using *only the two dimensional* shape functions integrated over surface **A**.

$$k_{ij} = c \int_{\text{surface A}} S_i S_j dx dy \quad (6)$$

Since the shape functions on the surfaces are assumed to be from conventional three dimensional finite elements, they satisfy the property that

$$S_1(x,y) + S_2(x,y) + \dots + S_m(x,y) = 1 \quad (\text{all } x,y \text{ on surface } \mathbf{A})$$

and

$$S_{m+1}(x,y) + S_{m+2}(x,y) + \dots + S_n(x,y) = 1 \quad (\text{all } x,y \text{ on surface } \mathbf{B})$$

These identities ensure that some basic properties of the conductance element are satisfied.

Mainly, symmetry and that the columns add to zero. In addition, they ensure that the total heat transferred between the surfaces is always correctly calculated.

For the case of a *direct coupling* between the surfaces, the contact resistance element with an artificially high conductance could offer an approximate solution. However, a much better approach is to constrain the temperatures on the contact surfaces to be as close as possible by minimizing a least-squares criterion E.

$$E = \int_{\text{SurfaceA}} [\text{Ta}(x,y) - \text{Tb}(x,y)]^2 dx dy \quad (7)$$

This error can be minimized by taking the partial derivative with respect to each node on surface A and setting it to zero. This operation leads to the identical set of equations found in a portion of the general contact finite element, Equation (2), mainly

$$\mathbf{K}_{11} \mathbf{T}_a + \mathbf{K}_{12} \mathbf{T}_b = \mathbf{0} \quad (8)$$

This leads to the constraint equation

$$\mathbf{T}_a = \mathbf{K}_c \mathbf{T}_b \quad \text{where} \quad \mathbf{K}_c = -\mathbf{K}_{11}^{-1} \mathbf{K}_{12} \quad (9)$$

A general Galerkin's approximation to the decoupled set of matrix-vector differential equations incorporating the above constraint gives the final set of differential equations. More details can be found in Reference [1]. Thus the integrals, Equations (6), are used for both direct coupling as well as for the contact resistance element.

In the above equation (9), the surface A is designated as the slave surface and surface B is the master surface. It is also possible to choose surface B as the slave surface, resulting in a similar constraint equation. This paper will not investigate which choice is better except to note that, intuitively, the smaller surface should be the slave surface.

3.0 Numerical Integration

The components of the conductance matrix, Equations (6), are to be evaluated numerically. In Reference [1], the mesh of the smaller surface was used to perform this integration. For very simple cases this would suffice. However, in a more practical setting this technique would result in some miscalculations. The objective of the method in this paper is to numerically integrate these integrals exactly. It is easy to imagine practical models with very complicated arbitrary meshes on both surfaces, both in number, distribution, and polynomial degree. Thus the method used for the integration of the integrals must be robust enough to take into account the complexities of both surface meshes.

One method, which is the one explored herein, is to construct a triangular mesh just to perform the numerical integration. With the choice of a triangle mesh it is possible to use Gaussian integration formulas to exactly integrate polynomial functions of various degrees. For example, a seven point formula will exactly integrate a polynomial of degree 5. The restriction is that the polynomial function must be continuous within the triangle. The objective is create a triangular mesh such that each triangle falls entirely within elements on both surfaces, thus ensuring the continuity of the shape functions within the integration triangle and the exact numerical integration of equations (6).

One method used to construct such a mesh is the constrained Delaunay triangulation method[8]. This method accepts nodes and specified segments and constructs a quality mesh. This method was applied to this problem in the following simple manner. First, a surface was chosen as a starting mesh, usually the smaller of the two. Any quadrilateral on this surface was divided into two triangular elements, thus producing a complete set of triangular elements that satisfy the continuity requirement for this surface. For each triangle on this surface the elements

on the other surface were searched to find all nodes that fell within and all points resulting from intersecting edges. This information was used, with constraints to preserve the original triangle, to construct a Delaunay triangular mesh. Any triangles formed outside of the original triangle were then discarded. The resulting mesh then satisfies the continuity requirements for both surfaces, and the numerical integration is performed over this triangular mesh. Note that this does not change the functions S_i which are determined solely by the meshes on each of the original surfaces. The two dimensional shape functions $S_i(x,y)$ are easily evaluated at any point (x,y) on a surface by setting T_i to unity and all the other nodal temperatures to zero. The resulting conductance matrix will have the usual properties expected of any conductance matrix, namely symmetry and the requirement that the columns add to zero.

This method will rely on the robustness of the Delaunay triangulation to construct the mesh and its ability to handle arbitrary nodal locations and the constraints. The next sections demonstrate the effectiveness of the method.

4.0 Simple Example of Dissimilar Meshes

As a demonstration of the ideas presented above consider one of the simplest examples of a connection between dissimilar meshes as shown in Figure 2. It consists of two surfaces with triangular elements on unit squares. Although the nodes align perfectly, the diagonals are connected to different pairs of nodes, thus producing the dissimilar meshes. The basis functions for these elements can produce different temperature fields even if the nodal temperatures on the opposite surface are identical.

Among the requirements for connecting dissimilar meshes is that the overall heat transferred between the surfaces be computed correctly. The overall heat being transferred

between the surfaces is

$$Q = c \int_{\text{Area}} (T_{\text{surface 1}}(x,y) - T_{\text{surface 2}}(x,y)) dx dy \quad (10)$$

For this example it is possible to analytically integrate the above integral and express it in terms of the nodal temperatures:

$$Q_{\text{exact}} = c/6 [2T_1 + T_2 + 2T_3 + T_4 - T_5 - 2T_6 - T_7 - 2T_8] \quad (11)$$

In the previous paper, Reference [1], the mesh on one of the surfaces would have been used to perform the numerical integration for the contact conductance matrix, Equations (6). An inspection of the meshes in Figure 2 shows that a numerical integration using either of the surface meshes will produce incorrect results. As mentioned above, the Gaussian numerical integration formulas are exact for certain polynomials but in this case there is not a continuous polynomial function since the opposite diagonal will cross any triangle chosen for the integration.

One mesh that will produce correct integrations is shown in Figure 3. For each triangle in this mesh the polynomial functions represented in the integrals are continuous. A seven point integration formula will properly integrate a fifth degree polynomial which is sufficient for simple triangles and quads. Using this integration mesh the contact conductivity matrix is calculated as (all terms multiplied by c and 2.08333E-02)

1	2	3	4	5	6	7	8	
-8.0	-2.0	-4.0	-2.0	5.0	5.0	1.0	5.0	1
	-4.0	-2.0	0.0	1.0	5.0	1.0	1.0	2
		-8.0	-2.0	1.0	5.0	5.0	5.0	3
			-4.0	1.0	1.0	1.0	5.0	4

(symmetric)	-4.0	-2.0	0.0	-2.0	5
		-8.0	-2.0	-4.0	6
			-4.0	-2.0	7
				-8.0	8

Now if all the heat transferred to the nodes on surface 1 are added using the above matrix the overall heat transferred is exactly equal to the analytical result in Equation (11), which assures that the overall heat transferred is being computed correctly.

Furthermore the constraint Equation (9) for direct coupling is calculated as

$$T_1 = 0.75 T_5 + 0.25 T_6 - 0.25 T_7 + 0.25 T_8$$

$$T_2 = T_6$$

$$T_3 = -0.25 T_5 + 0.25 T_6 + 0.75 T_7 + 0.25 T_8$$

$$T_4 = T_8$$

These constraint equation have a property that if the temperature distribution on one surface is linear ($a + bx + cy$) then the temperatures on the other surface match identically. This can be used as a further check on the numerical integration.

The proper integration mesh chosen for this simple example was obvious. The next sections demonstrate how the automatic generation of the integration mesh is used to solve more complex models.

5.0 Example 2 – Direct Coupling

This example demonstrates that the method used to directly couple dissimilar meshes does not degrade the solutions that would be obtained with comparable uniform mesh models. The test model is a unit cube with a lower corner at the origin and with the exact solution

$$T(x,y,z) = 64 x y z (1-x) (1-y) (1-z)$$

The heat distribution f is obtained by differentiating the above equation and satisfying

$$T_{xx} + T_{yy} + T_{zz} = -f$$

The dissimilar models were then constructed by connecting two portion of the cube both modeled with 8 node hexahedrons. One portion is constructed with a uniform mesh for the region from $z=0$ to 0.75 . The second portion used a different size uniform mesh for the region from $z=0.75$ to 1.00 . Several models were constructed by dividing the edges uniformly with $1/4$, $1/8$, $1/16$, and $1/32$ increments. Each portion would use different increments. A complete model with a (16,8) edge increment combination is shown in Figure 4. The surfaces at the interface ($z=0.75$) were connected using the above constraint method for direct coupling.

In order to evaluate the possible additional errors caused by connecting dissimilar grids, a comparison was made with several finite element models of 8 node hexahedrons with uniform grids for the entire model. The models were constructed by dividing the edges uniformly with $1/4$, $1/8$, $1/16$, and $1/32$ increments. The least square errors (L2) between the exact solution and the uniform mesh finite element nodes are shown in Figure 5 versus the total number of nodes in the models.

The L2 errors between the exact solution and the dissimilar models are shown in Figure 5 for the edge combinations (4,8), (8,4), (8,16), (16,8), (16,32). and (32,16). As the figure shows the errors only slightly greater than those with a complete uniform mesh. Also, the errors are decreasing at the same rate as those of the uniform mesh which means that direct coupling method for connecting dissimilar meshes produces the same convergence rate as uniformly meshed models.

6.0 Example 3 – Contact Resistance Element

In order to further illustrate the method for generating the integration mesh using Delaunay triangularization, a more complex three dimensional model consisting of two vastly dissimilar meshes will be connected with a contact resistance. The model consists of a block connected to a hollow cylinder. The block is 2x4x1 units and the hollow cylinder has an inner radius of 0.2 units and an outer radius of 1 and is 1 unit in length. The cylinder is to be connected to the center of one of the larger faces of the block. Unit material properties are used. The boundary conditions for this example are to set the top and bottom faces of the block at 100 and the opposite face of the cylinder at 0. This creates a set of symmetries that will permit the use of a one-quarter model which is shown in Figure 6. In this rather simple case, the block is naturally meshed with uniform cubes while the cylinder lends itself to a mesh more reflecting its nature. This however, produces a rather complex dissimilar mesh at the interface. Two models were investigated, the first as shown in Figure 6, had a total of 305 nodes (model 1). A second, more refined model, had 3432 nodes (model 2).

The smaller of the two connecting surfaces in this model is the face of the cylinder. The elements on this face were used as the starting point for the integration mesh. The quadrilateral elements on the face were first divided into triangles and then the method outlined above was used to construct a mesh using Delaunay triangles. The resulting meshes are shown in Figures 7 and 8 for the two models, respectively. As these figures show, the requirements set for the exact integration of the contact matrix produces some rather complex meshes. The methodology for creating Delaunay triangularization is quite mature and handled these cases easily. These meshes were then used to numerically integrate the contact matrix together with a seven point integration formula for each of the triangles [7]. A seven point formula will exactly integrate polynomials

up to fifth degree which is sufficient for the product of triangle and quadrilateral elements.

Since this problem does not have an analytical solution it is difficult to measure the accuracy of the solution. One important measure is the total heat flux from the one face at 100 to the other at 0, also called the shape factor. The table below shows this heat flux for various values of c , the coefficient of thermal resistance.

Table 1 Total Heat Flux for various Coefficients

c	Qmodel1	Qmodel2
0.1	5.86	6.08
1.0	22.04	22.60
10.	30.73	31.31
100.	32.21	32.70
1000.	32.61	32.89
direct coupling	32.31	32.86

The heat flux for the larger values of c approximates the heat flux for a direct coupling (perfect connection). These results give confidence that the numerical calculations are correct.

7.0 Conclusions

A method for connecting independently three dimensional models either directly or with a contact resistance element has been investigated and found to perform very well. The robustness of the Delaunay triangulation in constructing the integration mesh has been demonstrated. The method is straightforward and could easily be added to any existing finite element heat conduction program. One goal for the practical use of this method is to provide a basis for creating archives of previously meshed components and accelerating analysis efforts by

simply connecting these components without having to readjust node locations or element types.

References:

- [1] D. M. Trujillo and C. G. Pappoff . A general thermal contact resistance finite element. *Finite Elements in Analysis and Design*, vol. 38, pp. 263-276, 2002.
- [2] F. B. Belgacem and Y. Maday. The Mortar Element Method for Three Dimensional Finite Elements, *RAIRO Model. Math. Anal. Numer.*, vol 31, pp. 289-302, 1997.
- [3] D. Arnold, F. Brezzi, B. Cockburn, and L.D. Marini. Unified Analysis of Discontinuous Galerkin Methods for Elliptic Problems, *SIAM J. Numer. Anal.*, vol 39, pp. 1749-1779, 2002.
- [4] C. R. Dohrmann, S. W. Key, and M. W. Heinstein. Methods for connecting dissimilar three-dimensional finite element meshes, *International Journal for Numerical Methods in Engineering*, vol. 47, pp. 1057-1080, 2000.
- [5] R. Becker, P. Hansbo, and R. Stenberg . A finite element method for domain decomposition with non-matching grids. *Mathematical Modeling and Numerical Analysis*, vol. 37, pp. 209-225, 2003.
- [6] J. B. Ransom, "A Multifunctional Interface Method for Coupling Finite Element and Finite Difference Methods: Two-Dimensional Scalar-Field Problems", 43rd AIAA/ASME/ASCE/AHS/ASC Structures, Structural Dynamics, and Materials Conference, Denver, Colorado, AIAA 2002-1573, April 22-25, 2002, pp. 13.
- [7] D. W. Pepper and J. C. Heinrich, The Finite Element Method, Taylor & Francis, Bristol, Pennsylvania, 1992.
- [8] J. R. Shewchuk, Delaunay Refinement Algorithms for Triangular Mesh Generation, *Computational Geometry Theory and Applications*, vol. 22, pp, 21-74, May 2002.

NOMENCLATURE

$T(x,y,z)$	Temperature distribution in the contact element
$T_a(x,y)$	Temperature distribution on Surface A
$T_b(x,y)$	Temperature distribution on Surface B
c	coefficient of thermal resistance
$N_i(x,y,z)$	General Three dimensional shape function
m	Number of nodes on surface A
n	Total number of nodes on surfaces A and B
$S_i(x,y)$	Two dimension shape function on A or B
A_e	Area of an element

Vectors and Matrices

K	Contact Resistance Element
T_a	Nodes on surface A , contact surface of model 1
T_b	Nodes on surface B , contact surface of model 2
K_{11}, K_{12}, K_{22}	Submatrices of K
k_{ij}	i th row, j th column entry of K

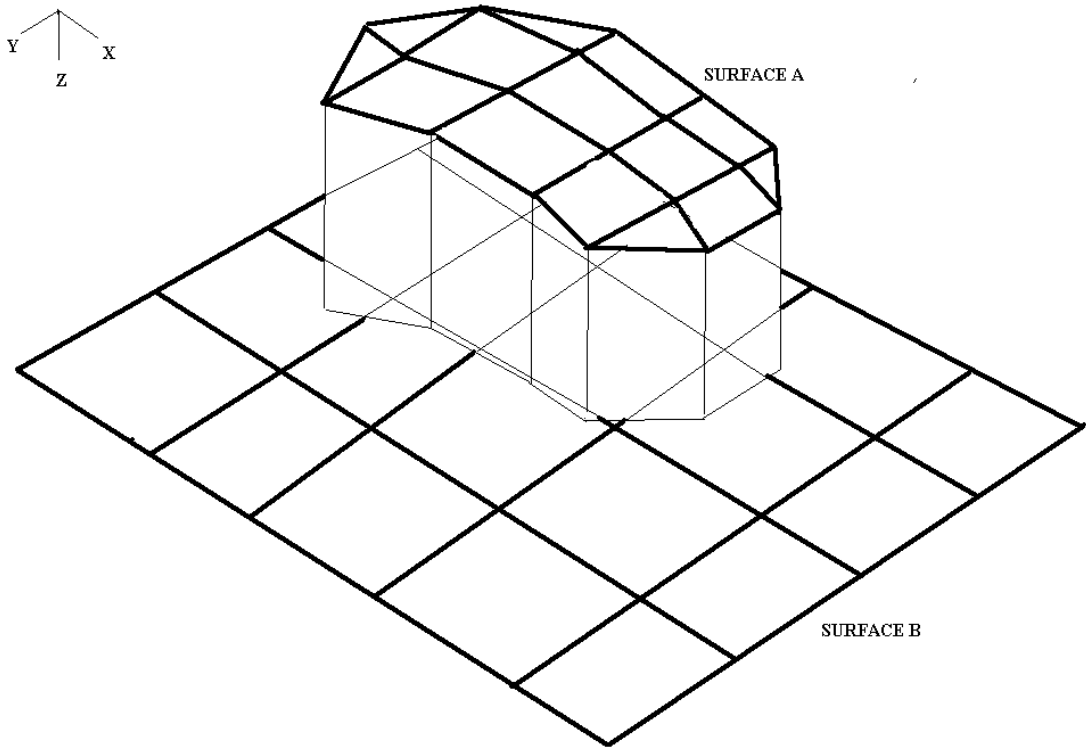


Figure 1 General Contact Resistance Element

Figure 2 Simple Example of Dissimilar Mesh

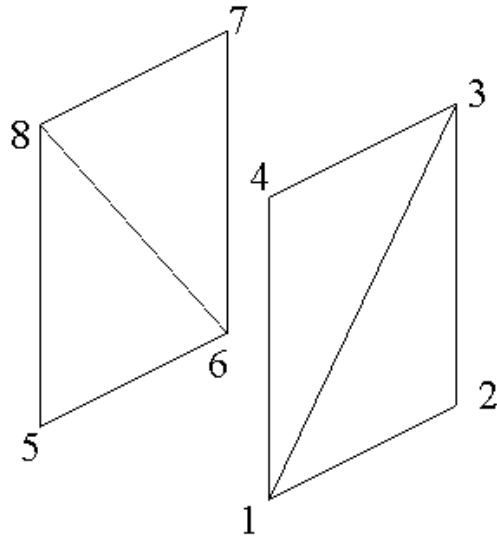


Figure 3 Integration Mesh for Simple Dissimilar Example

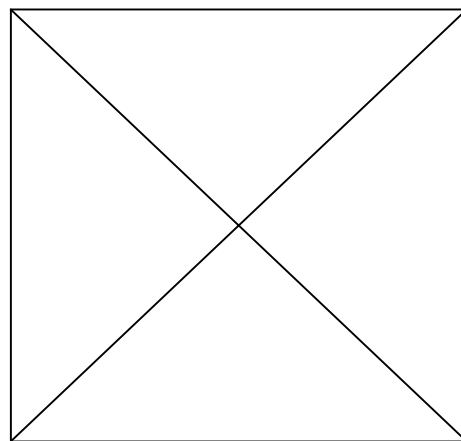


Figure 4 Mesh for a(16,8) Dissimilar Model

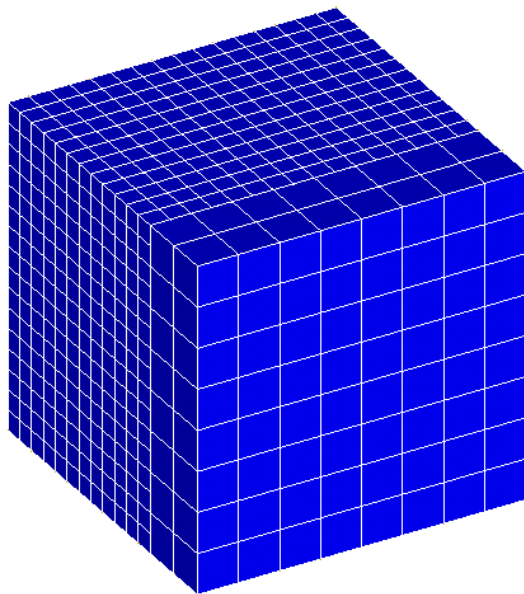


Figure 5 L2 Error vs Number of Nodes

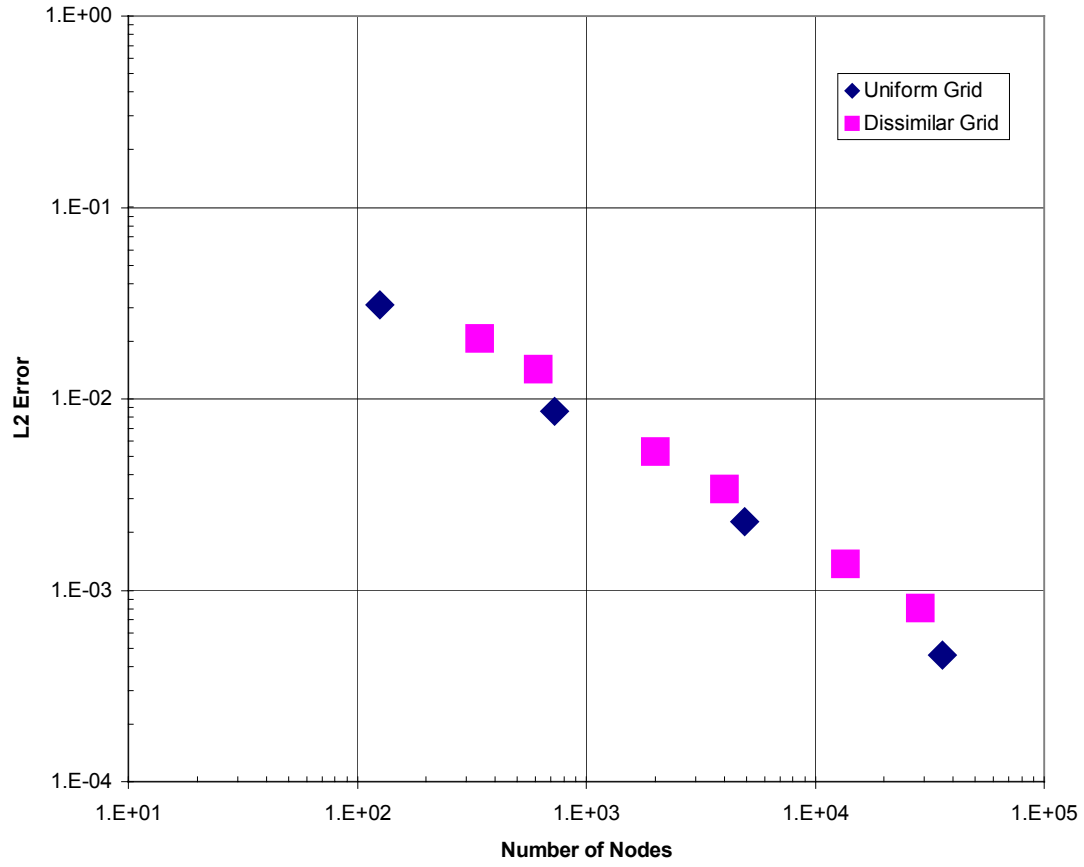


Figure 6 One-Quarter Model - Example 3

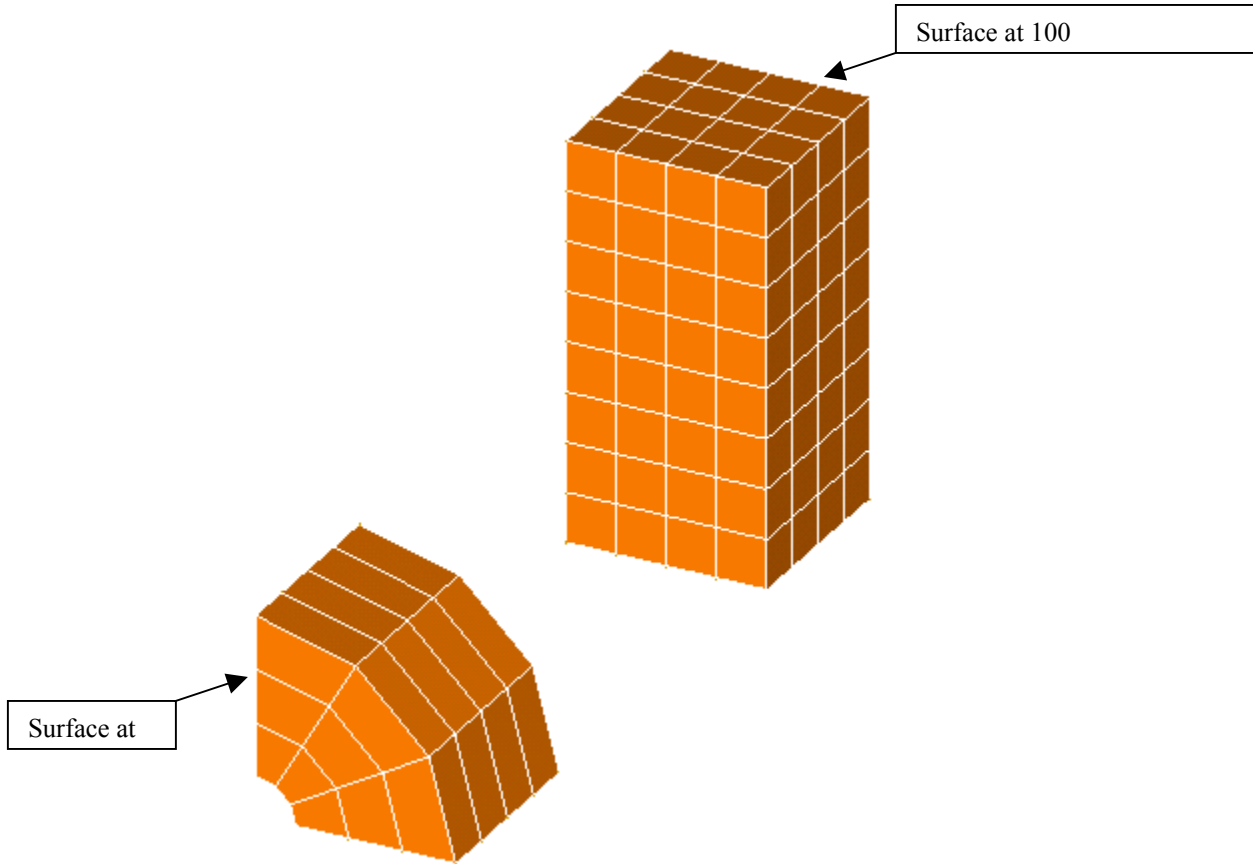


Figure 7 Delaunay Integration Mesh – Example 3, Model 1

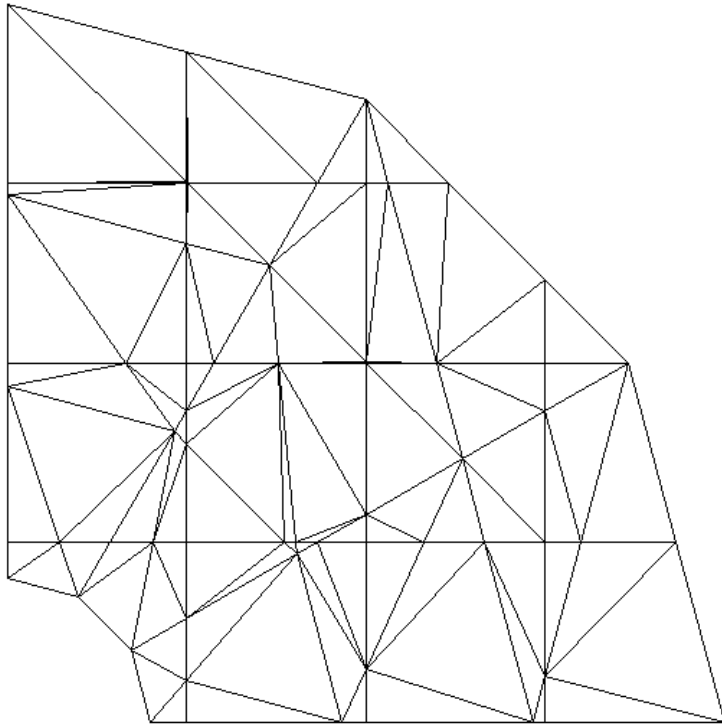


Figure 8 Delaunay Integration Mesh – Example 3, Model 2

